



# Imaging features and clinical significance of atypical pleural plaques mimicking bone tumors: a retrospective case series

Yeoun Eun Sung<sup>1^</sup>, Dae Hee Han<sup>2^</sup>, Kwanyong Hyun<sup>3^</sup>, Joon-Yong Jung<sup>2^</sup>, Suyon Chang<sup>2^</sup>

<sup>1</sup>Department of Hospital Pathology, Seoul St. Mary's Hospital, College of Medicine, The Catholic University of Korea, Seoul, Republic of Korea; <sup>2</sup>Department of Radiology, Seoul St. Mary's Hospital, College of Medicine, The Catholic University of Korea, Seoul, Republic of Korea; <sup>3</sup>Department of Thoracic and Cardiovascular Surgery, St. Vincent's Hospital, College of Medicine, The Catholic University of Korea, Seoul, Republic of Korea

*Correspondence to:* Suyon Chang, MD, PhD. Department of Radiology, Seoul St. Mary's Hospital, College of Medicine, The Catholic University of Korea, 222 Banpodaero, Seocho-gu, Seoul 06591, Republic of Korea. Email: ohyes723@gmail.com.

**Abstract:** This study aimed to examine the imaging characteristics and clinical implications of atypical pleural lesions that mimic bone tumors and form along the inner margins of consecutive ribs. This retrospective analysis included 45 atypical pleural lesions arising from 13 patients who underwent chest computed tomography (CT) between April 2021 and March 2023. The clinical features, CT findings, and radiologic diagnoses prior to pathologic identification were examined. Pathological findings were reviewed in the surgically resected case. Subgroup analysis was performed based on the presence of concurrent typical pleural plaques. The mean age of the patients was 69.3±8.4 years with a predominance of males (76.9%). The lesions primarily exhibited unilateral involvement (84.6%), being most frequently located in the right mid-level posterior region. Calcification was present in 75.6% of cases, typically seen continuously along the ribs (82.4%). Adjacent rib changes were observed in 28.9% of cases. These lesions were frequently misdiagnosed as osteochondromas or bony spurs (55.6%) by thoracic radiologists. No significant growth was observed during follow-up (n=11, 47±41 months), and the pathological findings were consistent with pleural plaques. Patients with concurrent typical pleural plaques had more atypical pleural lesions without statistical significance (P=0.071) and showed a more even distribution (P=0.039). In conclusion, atypical pleural lesions resembling bone tumors along consecutive ribs represent a distinct subset of pleural plaques. Their unique distribution and morphology should be recognized by radiologists to avoid misinterpretation and unnecessary interventions.

**Keywords:** Pleura; tomography; X-ray computed; diagnosis; differential

Submitted May 23, 2023. Accepted for publication Sep 13, 2023. Published online Sep 25, 2023.

doi: 10.21037/qims-23-725

**View this article at:** <https://dx.doi.org/10.21037/qims-23-725>

## Introduction

Pleural lesions encompass a wide range of etiologies, from benign to malignant, including tumors and tumor-like conditions (1). Various entities, such as solitary fibrous tumors of the pleura, lipomas, malignant mesotheliomas,

pleural lymphomas, pleural sarcomas, and pleural metastasis, fall under the umbrella of pleural tumors. In contrast, non-tumorous pleural lesions consist of pleural plaque, thoracic splenosis, and pleural pseudotumors, among others (2-4). Accurate diagnosis of pleural lesions is essential for optimal

<sup>^</sup> ORCID: Yeoun Eun Sung, 0000-0002-9408-0085; Dae Hee Han, 0000-0002-5239-9207; Kwanyong Hyun, 0000-0002-2103-3122; Joon-Yong Jung, 0000-0002-6909-0919; Suyon Chang, 0000-0002-9221-8116.

patient management and prognosis. However, determining the origin of a pleural lesion can be challenging, given the close relationship between the pleura, lung, and chest wall. Juxtapleural lesions may arise from osseous structures, cartilage, soft tissue, muscles, nerves, or fat (3).

In clinical practice, we have noted atypical pleural lesions exhibiting a unique morphology and distribution along the inner margin of consecutive posterior ribs, which are occasionally incidentally discovered on chest computed tomography (CT). Although typical pleural plaques present as bilateral, multifocal band-like lesions caused by localized pleural thickening and have a thin layer of fat separating them from the underlying ribs and extrapleural soft tissues (5-7), these atypical pleural lesions predominantly appear on the right posterior ribs and manifest as bony protrusions from the rib with soft tissue density. At our institution, interpretation of these lesions varied according to the radiologist's judgment. A literature search identified only one similar case report (8), with no studies describing the systematic analysis of multiple cases of these lesions.

Therefore, we conducted this study to collect data on these atypical pleural lesions, characterize their imaging features, and determine their clinical significance, ultimately establishing a consistent strategy for their interpretation and management.

## Methods

The study was conducted in accordance with the Declaration of Helsinki (as revised in 2013). The study was approved by the Institutional Review Board of Seoul St. Mary's Hospital (IRB No. KC23RISI0214) and informed consent was waived due to the retrospective nature of the study.

### *Study participants*

Over a 2-year period, a thoracic radiologist (Han DH) incidentally identified four sporadic cases of atypical pleural lesions during clinical practice. One of these cases was surgically confirmed in April 2021. Subsequently, all thoracic radiologists at the institution shared information regarding these lesions. Another thoracic radiologist (Chang S) systematically gathered and documented all patients presenting with atypical pleural lesions seen during clinical practice between April 2021 and March 2023. During this timeframe, 12 chest CT scans from nine patients with atypical pleural lesions were identified from a total

of 17,433 chest CT scans (0.07%). Ultimately, 45 atypical pleural lesions in 13 patients were included in this study.

### *Clinical characteristics*

We conducted a retrospective review of the electronic medical records from our hospital. Demographic and clinical data, including age, sex, height, weight, body mass index (BMI), smoking history, and asbestos exposure history, were recorded. Patients with positive asbestos exposure were defined as those who worked or lived near an asbestos mine, near a factory manufacturing asbestos products, near a train station transporting asbestos, or were employed in asbestos mining, asbestos-related product manufacturing, construction, transportation, unloading, or other areas where exposure to asbestos was likely (7). Furthermore, we recorded the presence of comorbid diseases, including malignancy, pneumoconiosis, treatment history of pulmonary tuberculosis, and interstitial lung disease.

### *Chest CT acquisition*

All participants underwent a CT examination with multidetector CT scanners ( $\geq 64$  channels), including Somatom Force (Siemens Healthineers, Erlangen, Germany), Somatom Definition AS+ (Siemens Healthineers), or GE Discovery CT750 HD (GE Healthcare, Milwaukee, WI, USA) at the end of inspiration during a single breath-hold. All CT scans were obtained with the following parameters: tube voltage 100–120 kV, tube current 30–200 mAs, pitch 0.984–2, rotation time 0.5 s, and detector collimation 0.6–0.625 mm. Axial images were reconstructed using a sharp kernel with a 1- or 1.25-mm section thickness. Coronal and sagittal images were reconstructed with 3-mm section thickness. All scans were obtained from the upper level of the lower neck to the level of the adrenal glands. Dose modulation was applied using automatic exposure control.

### *Image analysis*

Chest CT scans from 13 patients, performed between May 2012 and March 2023, were evaluated by consensus of two thoracic radiologists (Han DH and Chang S). For image analysis, the most recent chest CT was used, except when assessing interval changes in lesions.

Atypical pleural lesions were characterized as single or multiple pleural soft tissue density lesions with or without calcification, originating from the inner margins

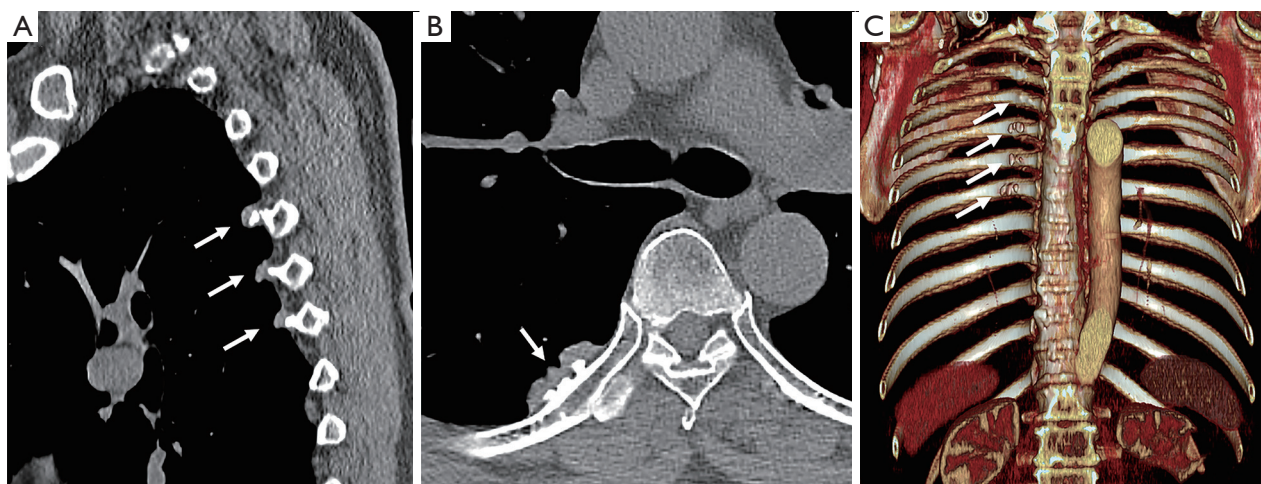


**Figure 1** Chest CT images in a 71-year-old man with atypical pleural lesions. (A) Sagittal and (B) axial CT images show consecutive atypical pleural lesions (arrows) along the right fourth to seventh posterior ribs (a small plaque at the right fourth rib is not clearly visible in this figure). Calcifications are seen in continuity with adjacent ribs, resembling bone lesions. (C) The three-dimensional volume rendering image also visualizes the atypical pleural lesions (arrows) along the right posterior ribs. CT, computed tomography.

of consecutive ribs (*Figure 1*). The following CT findings of atypical pleural lesions were analyzed on a per-patient and per-lesion basis: laterality (right *vs.* left), cranio-caudal location (adjacent rib level), anterior-posterior location, presence of calcification, apparent contiguity of the calcification with the adjacent rib, maximum length and width on axial plane images, and presence of adjacent rib changes (cortical thickening or widening). Concurrent typical pleural plaques or lung lesions suggestive of asbestos exposure, such as subpleural dot-like or branching opacities, curvilinear lines, band-like opacities (9), and round atelectasis (10), were also assessed. The presence of emphysema was also evaluated.

For patients with chest CTs preceding the surgical recognition of this pathology (*i.e.*, before April 2021), the initial radiological diagnosis was documented. In cases with multiple chest CT scans, follow-up duration and interval changes in lesions were examined. Six patients underwent  $^{18}\text{F}$ -fluorodeoxyglucose (FDG) positron emission tomography (PET)/CT scan, and significant FDG uptake in atypical pleural lesions was recorded based on PET/CT images by a radiologist (Chang S).

### ***Surgical resection and pathologic examination***

To rule out potential tumors, one patient underwent surgical resection. The excised pleura specimen was routinely fixed in 10% formalin solution, followed by gross dissection,

paraffin embedding, 4  $\mu\text{m}$  sectioning, and hematoxylin & eosin (H&E) staining. All H&E slides were reviewed by a thoracic pathologist (Sung YE).

### ***Statistical analysis***

Categorical variables are reported as raw numbers, proportions, and percentages, whereas continuous variables are presented as mean, standard deviation (SD), and range. Patient groups were categorized based on the presence of concurrent typical plaques for subgroup analysis. The chi-square test or Fisher's exact test was employed for categorical variables, and the independent *t*-test was used for continuous variables. The threshold for statistical significance was set at  $P < 0.05$ . Statistical analyses were performed using the SPSS software (version 24.0; IBM Corp., Armonk, NY, USA).

## **Results**

### ***Demographics***

*Table 1* presents the demographic information for the patients included in this study. The mean patient age was  $69.3 \pm 8.4$  (range, 53–81) years. Of the 13 patients, 10 (76.9%) were male, with the mean BMI being  $23.2 \pm 3.3 \text{ kg/m}^2$ . Eight patients (61.5%) were former smokers, whereas 4 (30.8%) were never smokers. The smoking history of 1 patient

**Table 1** Demographics of included 13 patients with atypical pleural lesions

Parameters	Value (n=13)
Age (years)	69.3±8.4 [53–81]
Sex	
Male	10 (76.9)
Female	3 (23.1)
Height (cm)	169.0±7.2
Weight (kg)	65.6±10.4
BMI (kg/m <sup>2</sup> )	23.2±3.3
Smoking history	
Never	4 (30.8)
Previous	8 (61.5)
Current	0 (0.0)
Unknown	1 (7.7)
History of asbestos exposure	
Yes	4 (30.8)
Unknown	9 (69.2)
Combined disease	
Malignancy	7 (53.8)
Pneumoconiosis	0 (0.0)
Treatment history of pulmonary tuberculosis	1 (7.7)
Interstitial lung disease	0 (0.0)

Values are presented as mean ± SD [range], n (%), or mean ± SD. BMI, body mass index; SD, standard deviation.

(7.7%) was unknown. A history of asbestos exposure was reported in 4 patients (30.8%), whereas 9 (69.2%) either had no confirmed asbestos exposure or were inadequately assessed. Combined malignancies were observed in 7 (53.8%) patients, and 1 (7.7%) had a history of pulmonary tuberculosis treatment. None of the patients had pneumoconiosis or interstitial lung disease.

#### *Atypical pleural lesions on a per-patient basis*

Table 2 provides a summary of the chest CT findings for patients exhibiting atypical pleural lesions. Among the 13 patients, 76.9% had multiple lesions, whereas 23.1% had a single lesion. The majority of patients (84.6%) had unilateral involvement, with the right side being affected more frequently than the left side (69.2% *vs.* 15.4%). All patients exhibited posteriorly located lesions, with 2 patients (15.4%) also presenting with lesions in the anterior thorax.

**Table 2** Chest CT findings of atypical pleural lesions on a per-patient basis

Parameters	Value (n=13)
Number of atypical pleural lesions	
1	3 (23.1)
2–4	7 (53.8)
≥5	3 (23.1)
Involvement of hemithorax	
Unilateral	11 (84.6)
Bilateral	2 (15.4)
Unilateral involvement (n=11)	
Right only	9 out of 11 (81.8)
Left only	2 out of 11 (18.2)
Dominant side	
Right	9 (69.2)
Left	2 (15.4)
Equal	2 (15.4)
Lesion location (anterior-posterior)	
Anterior only	0 (0.0)
Posterior only	11 (84.6)
Both	2 (15.4)
Concurrent typical pleural plaques	
Yes	4 (30.8)
No	9 (69.2)
Lung lesions to suggest asbestos exposure	
Yes	2 (15.4)
No	11 (84.6)
Emphysema	
Yes	4 (30.8)
No	9 (69.2)
Initial radiologic diagnosis (n=9) <sup>†</sup>	
Osteochondroma or bony spur	5 out of 9 (55.6)
Post-inflammatory change	1 out of 9 (11.1)
Not reported	3 out of 9 (33.3)
Patients with multiple chest CT scans (n=11)	
Follow-up duration (months)	47±41 [4–118]
Lesion growth during follow-up	
No	6 out of 11 (54.5)
Minimal	4 out of 11 (36.4)
More than minimal	1 out of 11 (9.1)

Values are presented as n (%) or mean ± SD [range], unless specified otherwise. <sup>†</sup>, CT reports made before the pathologic identification of this entity. CT, computed tomography; SD, standard deviation.

**Table 3** Distribution and CT characteristics of atypical pleural lesions on a per-lesion basis

Parameters	Value (n=45)
Involvement side	
Right	34 (75.6)
Left	11 (24.4)
Location (cranio-caudal)	
Upper (ribs 1–3)	6 (13.3)
Mid (ribs 4–7)	37 (82.2)
Lower (ribs 8–12)	2 (4.4)
Location (anterior-posterior)	
Anterior	3 (6.7)
Posterior	42 (93.3)
Calcification	
Yes	34 (75.6)
No	11 (24.4)
Apparent contiguity with adjacent rib (n=34)	
Yes	28 out of 34 (82.4)
No	6 out of 34 (17.6)
Maximum length <sup>†</sup> (mm)	12.6±8.5
Maximum width <sup>†</sup> (mm)	5.5±2.4
Adjacent bone change (cortical thickening or widening)	
Yes	13 (28.9)
No	32 (71.1)
Cortical thickening of adjacent ribs	
Yes	13 (28.9)
No	32 (71.1)
Widening of adjacent ribs	
Yes	10 (22.2)
No	35 (77.8)

Values are presented as n (%) or mean ± SD, unless specified otherwise. <sup>†</sup>, measured on axial plane images. CT, computed tomography; SD, standard deviation.

Concurrent typical pleural plaques were absent in 9 patients (69.2%), whereas 4 patients (30.8%) had combined typical pleural plaques. Within the latter group, 2 patients also had lung lesions suggesting asbestos exposure, including subpleural dot-like opacities (n=1) and round atelectasis (n=1). Emphysema was noted in four patients (30.8%).

Of the 13 patients, 9 (69.2%) had undergone chest CT scans before the pathology of atypical pleural lesion was identified through surgical resection in a single patient. Based on the chest CT findings, the initial diagnosis was osteochondroma or bone spur in 55.6% of these cases, and post-inflammatory change in 11.1%. In 33.3% of these cases, no lesions were reported. Among the 11 patients who underwent multiple CT scans, only one lesion exhibited significant interval growth during follow-up. This lesion demonstrated slow growth over a 6-year period (volume doubling time of 1,116 days), indicating a benign nature. The mean follow-up duration was 47±41 (range, 4–118) months.

### *Atypical pleural lesions on a per-lesion basis*

Table 3 and Figures 2,3 present the distribution and CT characteristics of atypical pleural lesions (n=45) on a per-lesion basis. The right hemithorax exhibited a higher frequency of lesion occurrence compared to the left hemithorax (75.6% vs. 24.4%). The majority of the lesions were located in the mid-level (fourth to seventh ribs, 82.2%, 37/45) and posterior thorax (93.3%, 42/45). The characteristic alignment of the right mid-level posterior ribs in a row was clearly visible in sagittal plane images (Figures 1,4). Calcification was present in 75.6% of lesions (34/45), with 82.4% demonstrating apparent contiguity with the adjacent rib (28/34). The maximum length and width of the atypical pleural lesions were 12.6±8.5 and 5.5±2.4 mm, respectively. Changes in the adjacent rib, such as cortical thickening or widening, were observed in 13 lesions (28.9%). Lesion size was largest at the mid-level (fourth to seventh ribs) in the craniocaudal direction, with conspicuous alterations in the adjacent ribs at this level (Figure 3). Of the six patients who underwent PET/CT, 22 atypical pleural lesions were identified, but none demonstrated significant FDG uptake.

### *Surgical and pathological findings*

Intraoperative findings for the patient who underwent surgical resection revealed multiple whitish protruding lesions along the right third to seventh posterior ribs (Figure 4C). These lesions originated from the parietal pleura rather than the visceral pleura or bone. The specimen comprised a single fragment of pleural tissue measuring 3.0 cm × 1.2 cm and was fully embedded in paraffin blocks. Microscopic examination revealed a “basket weave” collagen pattern fibrosis with focal calcification, predominantly acellular

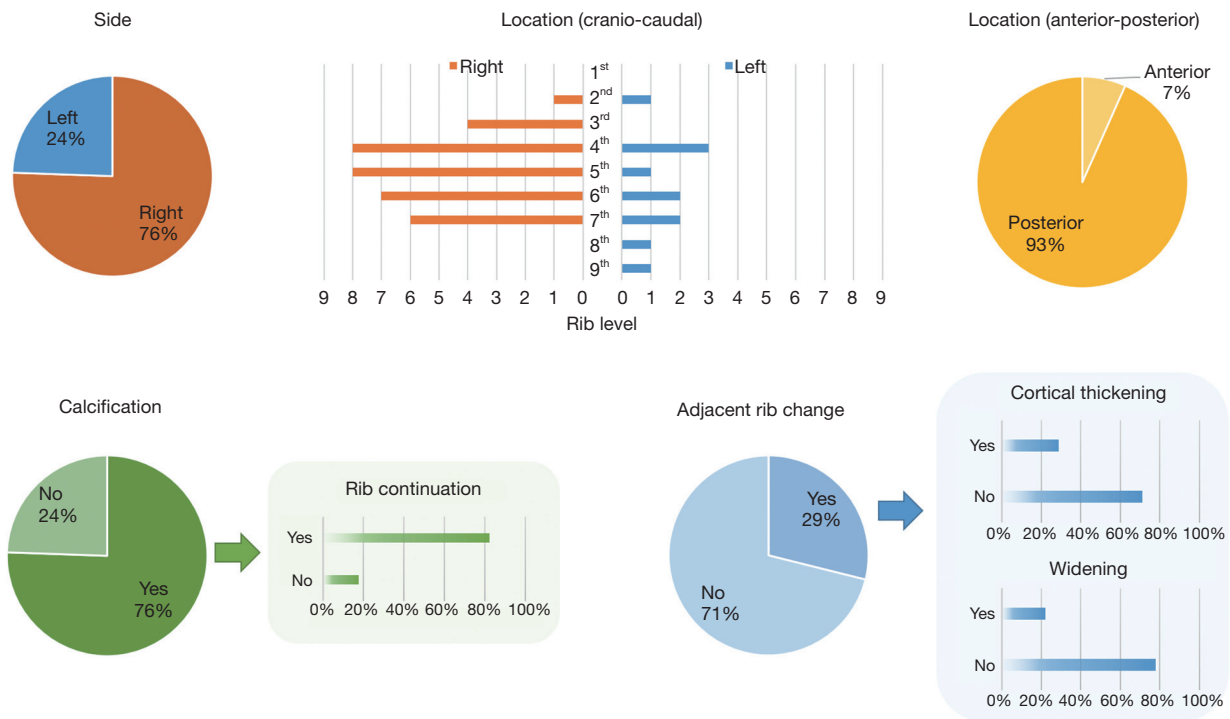


**Figure 2** Distribution and CT characteristics of atypical pleural lesions. Atypical pleural lesions were predominantly observed on the right side, mid-level between the fourth to seventh ribs, and in a posterior location. Internal calcifications were present in approximately 76% of the lesions, with most calcifications connected to the rib. Adjacent rib changes, such as cortical thickening or widening, were observed in about 29% of lesions. CT, computed tomography.

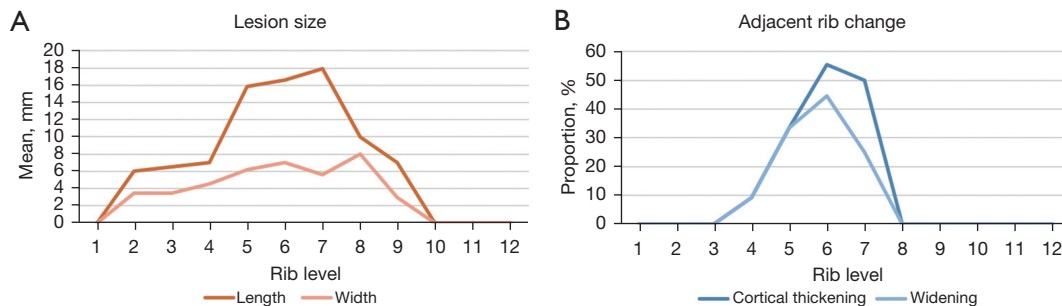


**Figure 3** Lesion size and adjacent rib changes in relation to the level of adjacent ribs. (A) The mean length and width of atypical pleural lesions were largest in the mid-level (from fourth to seventh ribs) of the thorax. (B) Adjacent rib changes, such as cortical thickening or widening, were also more frequently observed in the mid-level of the thorax compared to other regions.

but with occasional bland-appearing cells (Figure 4D,4E). Marked chronic inflammatory cell infiltration into the adherent adipose tissue beneath the parietal pleura was observed in multifocal areas at the base of the nodular pleural fibrosis. The specimen showed no evidence of asbestos.

**Subgroup analysis based on the presence of concurrent typical plaques**

Table 4 presents the results of a subgroup analysis based on the presence of concurrent typical plaques. All four patients with concurrent typical plaques were male (100%),

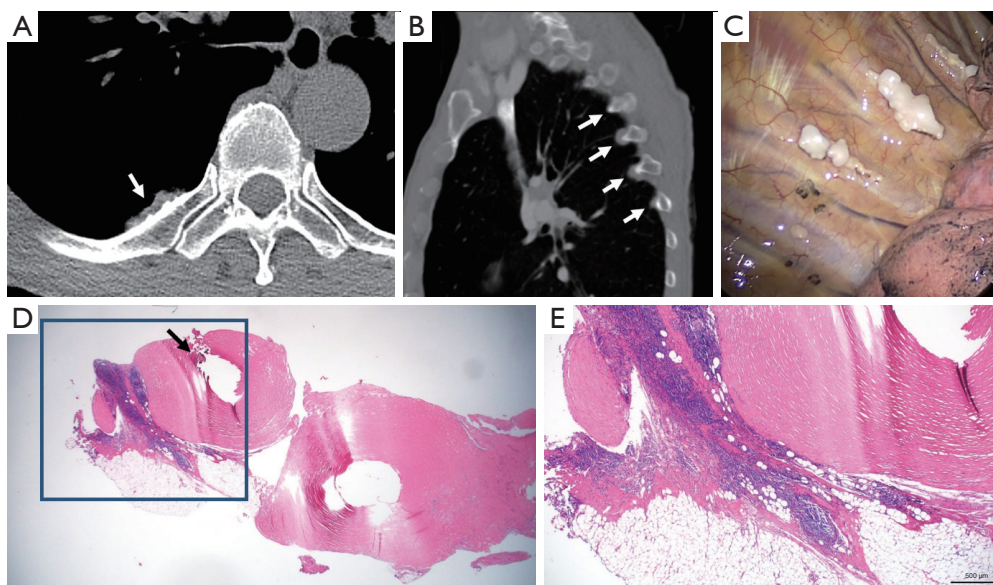


**Figure 4** Imaging, surgical, and pathologic findings of atypical pleural lesions in a 63-year-old man. (A,B) Axial and sagittal plane images of chest CT demonstrate consecutive atypical pleural lesions (arrows) along the right third to seventh posterior ribs (a small plaque on the right third rib is not clearly visible in this figure). Subtle cortical thickening and widening of the adjacent rib are also noted. (C) Surgical findings show multiple whitish protruding lesions along the right third to right seventh posterior ribs. They originate from the parietal pleura rather than the visceral pleura or bone. (D,E) Microscopic findings exhibit a “basket weave” collagen pattern fibrosis with focal calcification (arrow), which is mostly acellular but occasionally contains bland-appearing cells [H&E staining,  $\times 10$  (D),  $\times 50$  (E)]. These observations are consistent with the features observed in typical pleural plaques. Additionally, multifocal areas of marked chronic inflammatory cells infiltrating into the adherent adipose tissue beneath the parietal pleura are observed at the base of the nodular pleural fibrosis (D, square & E). CT, computed tomography. H&E, hematoxylin & eosin.

whereas only 66.7% of those without were male. Among the group lacking concurrent typical plaques, two patients had a known history of asbestos exposure but exhibited only atypical pleural lesions. In the group with concurrent typical plaques, two patients had a history of asbestos exposure, whereas the remaining patients’ exposure history was not fully assessed. Although the total number of atypical pleural lesions was higher in patients with typical pleural plaques than in the other group ( $5.0 \pm 2.6$  vs.  $2.8 \pm 1.5$ ), the difference was not statistically significant ( $P=0.071$ ). Right-side dominance was observed in 88.9% of patients without concurrent typical plaques, whereas the other group exhibited a relatively even distribution with 25% right-side dominance ( $P=0.039$ ). All lung lesions suggestive of asbestos exposure ( $n=2$ ) were found in patients with concurrent typical pleural plaques.

## Discussion

This study aimed to investigate the clinical and imaging

features, and pathologic findings of atypical pleural lesions and determine their clinical significance and management strategies. Our results indicate that these lesions were often detected on chest CT scans and more frequently in older men (mean age of 69.3 years). However, thoracic radiologists frequently misdiagnose these lesions as osteochondromas, bony spurs, or pleural metastasis (8), leading to potentially unnecessary diagnostic procedures, including follow-up CT, PET/CT, or even surgery. Therefore, it is necessary to analyze the characteristics and clinical significance of these less well-known lesions to provide guidance for radiologists.

Pleural plaques are often incidentally detected, and their differential diagnosis encompasses a wide range of entities, including extrapleural fat, pleural metastasis, malignant mesothelioma, pleural tuberculosis, and others (2,4). Unlike typical pleural plaques, which commonly present as bilateral, multiple lesions with frequent diaphragmatic involvement (7,11,12), atypical pleural lesions are characterized by unilateral involvement and a

**Table 4** Comparison between patients with or without concurrent typical pleural plaques

Parameters	Without concurrent typical plaques (n=9)	With concurrent typical plaques (n=4)	P
Age (years)	66.9±8.8	74.8±4.5	0.123
Sex (male)	6 (66.7)	4 (100.0)	0.497
Height (cm)	169.4±8.1	166.7±4.7	0.607
Weight (kg)	65.2±6.5	66.7±20.4	0.915
BMI (kg/m <sup>2</sup> )	23.0±2.4	23.8±5.9	0.850
Smoking status (ever) (known; n=12)	5 out of 8 (62.5)	3 out of 4 (75.0)	>0.999
History of asbestos exposure	2 (22.2)	2 (50.0)	0.530
Comorbid disease			
Malignancy	4 (44.4)	3 (75.0)	0.559
Treatment history of pulmonary tuberculosis	1 (11.1)	0 (0.0)	>0.999
Lesion number (categorical)			0.206
1	3 (33.3)	0 (0.0)	
2–4	5 (55.6)	2 (50.0)	
≥5	1 (11.1)	2 (50.0)	
Lesion number (continuous)	2.8±1.5	5.0±2.6	0.071
Unilateral involvement	9 (100.0)	2 (50.0)	0.077
Laterality (right)	8 out of 9 (88.9)	1 out of 2 (50.0)	0.345
Dominant side			0.039*
Right	8 (88.9)	1 (25.0)	
Left	1 (11.1)	1 (25.0)	
Equal	0 (0.0)	2 (50.0)	
Lesion location (anterior-posterior)			0.077
Posterior only	9 (100.0)	2 (50.0)	
Both	0 (0.0)	2 (50.0)	
Lung lesions to suggest asbestos exposure	0 (0.0)	2 (50.0)	0.077
Emphysema	2 (22.2)	2 (50.0)	0.530
Initial radiologic diagnosis <sup>†</sup> (n=9)	n=6	n=3	0.301
Osteochondroma or bony spur	4 out of 6 (66.7)	1 out of 3 (33.3)	
Post-inflammatory change	0 out of 6 (0.0)	1 out of 3 (33.3)	
Not reported	2 out of 6 (33.3)	1 out of 3 (33.3)	
Patients with multiple chest CT scans (n=11)	n=7	n=4	
Follow-up duration (months)	58.3±46.3	27.3±25.2	0.253
Lesion growth			0.104
No	3 out of 7 (42.9)	3 out of 4 (75.0)	
Minimal	4 out of 7 (57.1)	0 out of 4 (0.0)	
More than minimal	0 out of 7 (0.0)	1 out of 4 (25.0)	

Values are presented as mean ± SD or n (%), unless specified otherwise. \*, statistically significant; †, CT reports made before the pathologic identification of this entity. BMI, body mass index; CT, computed tomography; SD, standard deviation.

distinctive arrangement in a row with the right mid-level posterior dominance. Calcification within the lesions often appears continuous with the adjacent rib, and some cases exhibit alterations to the neighboring rib, such as cortical thickening or widening. These lesions exhibited stability over time, and the lack of significant uptake on PET/CT scans suggested a benign nature. Pathological findings from a resected case corresponded to the characteristics of pleural plaques. Therefore, a case displaying characteristic imaging features may not require additional diagnostic tests or interventions.

Mechanical stress-induced fibrosis has been proposed as the underlying cause of these atypical pleural lesions (8). In our study, they predominantly occur near the posterior rib tubercles, and the development of an atypical pleural lesion near a healed anterior rib fracture supports the theory that bone protrusion-associated friction may promote fibrosis. Pathological examination of the pleural tissue revealed a “basket weave” collagen pattern fibrosis, primarily acellular but occasionally with bland-appearing cells. These findings are consistent with the features observed in typical pleural plaques (13), corroborating previous reports (8). Interestingly, we also observed focal dense chronic inflammatory cell infiltration at the base of the parietal pleura, which is atypical compared to typical pleural plaques (14). The chronic inflammatory cell infiltration into the fat beneath the parietal pleura was accompanied by fibrosis. This inflammatory response might be accelerated by mechanical stimuli, as suggested by our initial hypothesis. Changes in the adjacent rib, such as cortical thickening and widening, are often observed in patients with pleural diseases and may reflect a chronic inflammatory process involving the pleura (15,16). Together, these findings suggest that atypical pleural lesions are likely the result of enhanced fibrosis in specific regions, such as the posterior rib tubercles or healed fractures, occasionally accompanied by periosteal reactions.

Determining whether these lesions result solely from asbestos exposure remains challenging. Pleural plaques are commonly associated with asbestos exposure, but other factors, including trauma and non-asbestos particle exposure, such as naturally occurring silicates, can also contribute to their development (17-19). Our study did not establish a clear association between typical pleural plaques and atypical pleural lesions, but we observed a slightly higher number of atypical pleural lesions in cases with concurrent typical pleural plaques. Moreover, two patients with a history of asbestos exposure presented solely with atypical pleural lesions and no typical plaques. These results

imply that both asbestos and other factors may contribute to pleural inflammation and fibrosis.

The limitations of this study include its retrospective design, small sample size, and limited pathological confirmation. Nevertheless, all included cases demonstrated the same distinctive imaging features without significant growth, and our results are consistent with previous reports (8), suggesting that these lesions likely represent the same pathology. The retrospective nature of the study also limited our ability to fully investigate smoking and asbestos exposure histories, potentially leading to an underestimation of asbestos exposure. Future research employing larger sample sizes and prospective designs is needed to further explore their association with asbestos exposure.

In conclusion, atypical pleural lesions represent a distinct subset of pleural plaques identifiable through their unique distribution and morphology. Radiologists should be aware of these lesions to avoid misinterpretation and unnecessary diagnostic work-up.

## Acknowledgments

*Funding:* None.

## Footnote

*Conflicts of Interest:* All authors have completed the ICMJE uniform disclosure form (available at <https://qims.amegroups.com/article/view/10.21037/qims-23-725/coif>). The authors have no conflicts of interest to declare.

*Ethical Statement:* The authors are accountable for all aspects of the work in ensuring that questions related to the accuracy or integrity of any part of the work are appropriately investigated and resolved. This study was approved by the Institutional Review Board of Seoul St. Mary's Hospital (IRB No. KC23RISI0214) and informed consent was waived due to the retrospective nature of the study.

*Open Access Statement:* This is an Open Access article distributed in accordance with the Creative Commons Attribution-NonCommercial-NoDerivs 4.0 International License (CC BY-NC-ND 4.0), which permits the non-commercial replication and distribution of the article with the strict proviso that no changes or edits are made and the original work is properly cited (including links to both the formal publication through the relevant DOI and the license).

See: <https://creativecommons.org/licenses/by-nc-nd/4.0/>.

## References

1. Sureka B, Thukral BB, Mittal MK, Mittal A, Sinha M. Radiological review of pleural tumors. *Indian J Radiol Imaging* 2013;23:313-20.
2. Walker CM, Takasugi JE, Chung JH, Reddy GP, Done SL, Pipavath SN, Schmidt RA, Godwin JD 2nd. Tumorlike conditions of the pleura. *Radiographics* 2012;32:971-85.
3. Desimpel J, Vanhoenacker FM, Carp L, Snoeckx A. Tumor and tumorlike conditions of the pleura and juxtapleural region: review of imaging findings. *Insights Imaging* 2021;12:97.
4. Bae JY, Kim Y, Kang HJ, Kwon H, Shim SS. Imaging Features of Various Benign and Malignant Tumors and Tumorlike Conditions of the Pleura: A Pictorial Review. *Taehan Yongsang Uihakhoe Chi* 2020;81:1109-20.
5. Peacock C, Copley SJ, Hansell DM. Asbestos-related benign pleural disease. *Clin Radiol* 2000;55:422-32.
6. Qureshi NR, Gleeson FV. Imaging of pleural disease. *Clin Chest Med* 2006;27:193-213.
7. Kim Y, Myong JP, Lee JK, Kim JS, Kim YK, Jung SH. CT Characteristics of Pleural Plaques Related to Occupational or Environmental Asbestos Exposure from South Korean Asbestos Mines. *Korean J Radiol* 2015;16:1142-52.
8. Kusakabe M, Kazaoka J, Hiyama N, Matsumoto J, Horiuchi H. Pleural nodule with osteal protrusion anterior to the rib tubercle: a case report. *Radiol Case Rep* 2021;16:2091-4.
9. Akira M, Yamamoto S, Inoue Y, Sakatani M. High-resolution CT of asbestosis and idiopathic pulmonary fibrosis. *AJR Am J Roentgenol* 2003;181:163-9.
10. Cugell DW, Kamp DW. Asbestos and the pleura: a review. *Chest* 2004;125:1103-17.
11. Rous V, Studený J. Aetiology of pleural plaques. *Thorax* 1970;25:270-84.
12. Matyga AW, Chelala L, Chung JH. Occupational Lung Diseases: Spectrum of Common Imaging Manifestations. *Korean J Radiol* 2023;24:795-806.
13. Cagle PT, Allen TC. Pathology of the pleura: what the pulmonologists need to know. *Respirology* 2011;16:430-8.
14. Roberts GH. The pathology of parietal pleural plaques. *J Clin Pathol* 1971;24:348-53.
15. Eyles WR, Monsein LH, Beute GH, Tilley B, Schultz LR, Schmitt WG. Rib enlargement in patients with chronic pleural disease. *AJR Am J Roentgenol* 1996;167:921-6.
16. Guttentag AR, Salwen JK. Keep your eyes on the ribs: the spectrum of normal variants and diseases that involve the ribs. *Radiographics* 1999;19:1125-42.
17. Scancarello G, Romeo R, Sartorelli E. Respiratory disease as a result of talc inhalation. *J Occup Environ Med* 1996;38:610-4.
18. Chaudhary BA, Kanis GJ, Pool WH. Pleural thickening in mild kaolinosis. *South Med J* 1997;90:1106-9.
19. Brown RC, Bellmann B, Muhle H, Davis JM, Maxim LD. Survey of the biological effects of refractory ceramic fibres: overload and its possible consequences. *Ann Occup Hyg* 2005;49:295-307.

**Cite this article as:** Sung YE, Han DH, Hyun K, Jung JY, Chang S. Imaging features and clinical significance of atypical pleural plaques mimicking bone tumors: a retrospective case series. *Quant Imaging Med Surg* 2023;13(12):8729-8738. doi: 10.21037/qims-23-725